Inorganic Chemistry

Article

pubs.acs.org/IC

Insights into the Molybdenum/Copper Heterometallic Cluster Assembly in the Orange Protein: Probing Intermolecular Interactions with an Artificial Metal-Binding ATCUN Tag

Biplab K. Maiti, Rui M. Almeida, Luisa B. Maia, Isabel Moura, and José J. G. Moura*

UCIBIO, REQUIMTE, Departamento de Química, Faculdade de Ciências e Tecnologia, Universidade Nova de Lisboa, 2829-516 Caparica, Portugal

Supporting Information

ABSTRACT: Orange protein (ORP) is a small bacterial protein, of unknown function, that contains a unique molybdenum/copper heterometallic cluster, $[S_2Mo^{VI}S_2Cu^{I}S_2Mo^{VI}S_2]^{3-}$ (Mo/Cu), non-covalently bound. The native cluster can be reconstituted in a protein-assisted mode by the addition of Cu^{II} plus tetrathiomolybdate to apo-ORP under controlled conditions. In the work described herein, we artificially inserted the ATCUN ("amino terminus Cu and Ni") motif in the *Desulfovibrio gigas* ORP ($Ala_1Ser_2His_3$ followed by the native amino acid residues; modified protein abbreviated as ORP*) to increase our understanding of the Mo/Cu cluster assembly in ORP. The apo-ORP* binds Cu^{II} in a 1:1 ratio to yield Cu^{II}-ORP*, as clearly demonstrated by EPR ($g_{\parallel,\perp}$ = 2.183, 2.042 and $A^{Cu}_{\parallel,\perp} = 207 \times 10^{-4}$ cm^{-1}, 19×10^{-4} cm^{-1}) and UV−visible spectroscopies (typical d−d transition bands at 520 nm, ε = 90 M^{-1} cm^{-1}). The ^{1}H NMR spectrum shows that His_3 and His_{53} are significantly affected upon the addition of the Cu^{II}. The X-ray structure shows that these two residues are very far apart (C_α−$C_\alpha \approx$ 27.9 Å), leading us to suggest that the metal-induced NMR perturbations are due to the interaction of two protein molecules with a single metal ion. Docking analysis supports the metal-mediated dimer formation. The subsequent tetrathiomolybdate binding, to yield the native Mo/Cu cluster, occurs only upon addition of dithiothreitol, as shown by UV−visible and NMR spectroscopies. Additionally, ^{1}H NMR of Ag^{I}-ORP* (Ag^{I} used as a surrogate of Cu^{I}) showed that Ag^{I} strongly binds to a native methionine sulfur atom rather than to the ATCUN site, suggesting that Cu^{II} and Cu^{I} have two different binding sites in ORP*. A detailed mechanism for the formation of the Mo/Cu cluster is discussed, suggesting that Cu^{II} is reduced to Cu^{I} and transferred from the ATCUN motif to the methionine site; finally, Cu^{I} is transferred to the cluster-binding region, upon the interaction of two protein molecules. This result may suggest that copper trafficking is triggered by redox-dependent coordination properties of copper in a trafficking pathway.

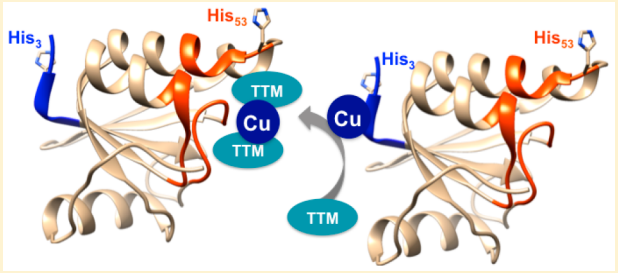

1. INTRODUCTION

Orange protein (ORP), first isolated from the sulfate-reducing organism *Desulfovibrio gigas*,[1] is found in several anaerobic bacteria.[2−4] It harbors a unique molybdenum/copper heterometallic cluster, $[S_2Mo^{VI}S_2Cu^{I}S_2Mo^{VI}S_2]^{3-}$ (Mo/Cu), revealed by EXAFS (Figure 1A).[1] The metal cofactor is stabilized in the binding pocket through non-covalent interactions,[5] but it does not involve any of the common metal-binding amino acid side chains, such as cysteine, histidine, and methionine side chains. Moreover, ORP can be heterologously expressed and isolated in an apo-form, which can be subsequently reconstituted in a protein-assisted mode using Cu^{II} and tetrathiomolybdate (TTM, MoS_4^{2-}) salts, to yield a reconstituted protein that is identical to the native holo-ORP.[5,6]

The biological function of ORP is still unknown; however, it is tempting to suggest that it may be related to its ability to "chelate" copper. Cells developed several copper sequestration and trafficking mechanisms to prevent the metal from reaching toxic levels, through which copper is scavenged and transferred by transient and specific protein−protein interactions, without dissociation of the "free" metal inside the cell.[7−10] In this context, TTM (part of the ORP Mo/Cu cluster) presents itself as an ideal "trap" for copper. Due to its reactivity with copper, TTM plays an antagonist role[11,12] toward many copper-containing[13,14] and copper-transferring proteins.[15,16] TTM reactivity has also been explored for management of Wilson's disease and other copper-dependent diseases, where the dietary supplementation of animal models with TTM allowed the observation of the formation of hepatic Mo/Cu clusters.[17−20] Yet, to our knowledge, in spite of this well-known chemistry, the Mo/Cu complex is unique to ORP, and its identification in the *D. gigas* ORP in 2000[1] was surprising.

Presently, the mechanism of the *in vivo* formation of the ORP Mo/Cu cluster is unknown; *in vitro*, the reconstitution of apo-ORP is achieved by the addition of Cu^{II} (1 equiv) followed by TTM (2 equiv), in a process where the order of Cu^{II} and TTM addition is critical to obtain a holo-ORP identical to the

Received: April 4, 2017
Published: July 25, 2017

DOI: 10.1021/acs.inorgchem.7b00840
Inorg. Chem. 2017, 56, 8900−8911

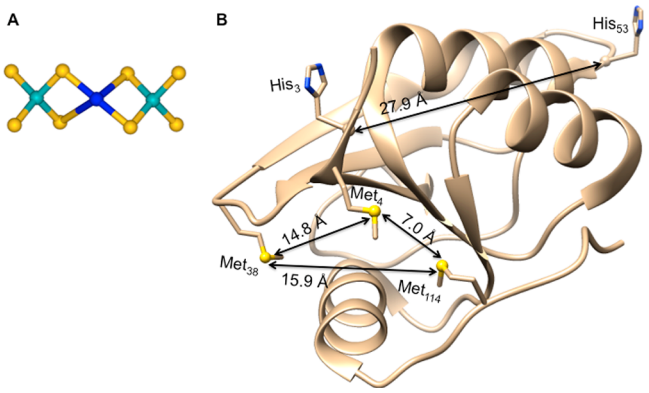

Figure 1. (A) Structure of the Mo/Cu cluster of ORP, as revealed by EXAFS[1] (sulfur, gold spheres; copper, blue sphere; and molybdenum, cyan spheres). (B) X-ray structure of *D. gigas* apo-ORP* (from PDB file 2WFB),[35] where key methionine and histidine residues are highlighted (with ORP* numbering), as well as the distances measured between sulfur atoms (golden sphere) and C_α atoms (gray sphere).

native protein. However, our understanding about the *in vitro* reconstitution of ORP has not yet been linked to the *in vivo* mechanism of Mo/Cu formation. In living organisms, Cu^{II} and Cu^{I} are preferentially sequestered by histidine- and methionine-rich protein regions, respectively.[21−23] The (H_2N)-$X_1X_2His_3$ motif, with a histidine in the third position, is a well-known high-affinity Cu^{II}-binding site, named ATCUN (from "amino terminus Cu and Ni"), that is found in several naturally occurring, biologically important, copper-binding proteins,[24−28] but not in ORP.

It is noteworthy that, due to its small size (causing minimal perturbation in protein structure and function), the ATCUN motif is perfectly suited to be artificially introduced into proteins for high-precision structure determination of intermolecular interaction studies, as the site for the introduction of paramagnetic probes.[29−32] The use of paramagnetic probes has proven to be very useful to obtain valuable structural information,[33] and the introduction of an ATCUN motif can be exploited to understand the ORP Mo/Cu cluster assembly process, as well as to obtain additional structural information about this intriguing protein.

In this work, we took advantage of the ATCUN motif, previously introduced into the *D. gigas* ORP sequence for cloning and purification purposes, by the addition of three residues to the *N*-terminus of the native protein sequence, $Ala_1Ser_2His_3$, followed by the native amino acid residues (modified protein hereafter abbreviated as ORP*). The crystal structure of apo-ORP* was previously determined (Figure 1B).[5,34,35] The reconstitution of the Mo/Cu cluster in ORP* from *D. gigas*[5] was not straightforward, and later it was modified[6] by addition of DTT, but the role of the metal-binding properties of this small ATCUN tag was overlooked. Recently, we also described a simple, straightforward method for reconstitution of other recombinant ORPs from *Desulfovibrio alaskensis* G20, where the ATCUN tag was absent.[4] In this simple process, Cu^{II} (free from ATCUN) is first reduced by TTM (cysteine is absent in both *D. alaskensis* and *D. gigas*), and finally TTM binds Cu^{I} to yield the native Mo/Cu cluster.

In biology, copper has two oxidation states (Cu^{I} and Cu^{II}), but *in vivo* it is not clear if copper is inserted into ORP as Cu^{II} and then reduced or directly inserted in the reduced form. Since the ATCUN tag prefers binding Cu^{II} over Cu^{I}, it would be helpful to understand this redox/insertion process. The protein containing a methionine coordinating site may play a relevant role when copper is reduced to Cu^{I} upon being released from the ATCUN to the methionine site without a dissociation pathway as observed in the copper trafficking pathway. As the Cu^{II} (ATCUN) and Cu^{I} (methionine) binding sites are opposite to the Mo/Cu cluster-binding region (His_{53}), we are motivated to understand the copper trafficking pathway to the formation of Mo/Cu cluster in ORP by taking advantage of a designed fusion protein, which mimics a protein−protein interaction.

The ATCUN tag's ability to coordinate Cu^{II} (Cu^{II}-ORP*) was thoroughly studied in the work described herein, using UV−visible, EPR, and ^{1}H NMR spectroscopies. The paramagnetic Cu^{II}-ORP* was exploited to determine the sites of metal−protein interaction from NMR spectroscopic studies. In addition, Ag^{I} was used as a probe (in place of Cu^{I}) to determine the monovalent metal−thioether (M^{I}-S-methionine) interaction by ^{1}H NMR. Since the X-ray crystal structure of the apo-ORP* is known (Figure 1B),[35] this allowed us to use computational methodologies to model protein−protein interactions and to discuss in detail the mechanism of copper binding to ORP.

2. MATERIALS AND METHODS

Unless otherwise stated, all reagents were of analytical or higher grade and were purchased from Sigma-Aldrich or Fluka.

2.1. General Procedure for the Reconstitution of Cu^{II}-ORP* and Ag^{I}-ORP* Derivatives. Fusion *D. gigas* protein, ORP*, was heterologously expressed in *Escherichia coli* BL21(DE3) and purified in the apo-form as previously described.[5,34] Subsequently, 1 mM $CuCl_2$ (or $AgNO_3$) was added to 1 mM apo-ORP* (in 50 mM Tris-HCl, pH 7.6, for Cu^{II} and 50 mM HEPES, pH 7.5 for Ag^{I}), and the mixture was incubated for 5 min on an ice bath (4 °C).

2.2. Assays of Cu^{II}-ORP* Reduction and Mo/Cu-ORP* Formation. The Cu^{II} reduction in Cu^{II}-ORP* was evaluated with TTM in the presence of dithiothreitol (DTT). TTM forms a $[Cu^{I}(MoS_4)_2]^{3-}$ cluster and exhibits characteristic absorption bands at 340 and 480 nm.[5,6] The reaction was monitored at room temperature in a 1 cm quartz optical cell, which contained 100 μM Cu^{II}-ORP* (a 1:1 mixture of $CuCl_2$ (100 μM) and apo-ORP* (100 μM)), 200 μM $(NH_4)_2MoS_4$, and 2 mM DTT over 2 h under air at room temperature. The absorbance bands at 340 nm (ε = 11 800 ± 750 M^{-1} cm^{-1}) and 480 nm (ε = 7850 ± 500 M^{-1} cm^{-1}) at a given time of reaction indicated conversion into the $[Cu^{I}(MoS_4)_2]^{3-}$ complex by the reduction of copper.[5,6] One set of samples was tested without DTT under similar conditions; their UV−visible spectrum at 317 and 469 nm (free TTM) does not shift any more over a period of 6 h.

2.3. Straightforward Method for Formation of $[Cu^{I}(MoS_4)_2]^{3-}$ in ORP*. To overcome the formation of a stable Cu^{II}-ATUCN complex, 1 mM DTT was added into 75 μM apo-ORP* in 1 mL of 50 mM Tris-HCl, pH 7.6, in a 1 cm quartz optical cell to generate a reducing environment, followed by addition of 75 μM $CuCl_2$ and 150 μM $(NH_4)_2MoS_4$ at RT. After this addition, the $[Cu^{I}(MoS_4)_2]^{3-}$ complex is formed immediately, as observed by the absorbance bands at 340 nm (ε = 12 000 ± 700 M^{-1} cm^{-1}) and 480 nm (ε = 8000 ± 400 M^{-1} cm^{-1}).

2.4. Reconstitution of $[Ag^{I}(MoS_4)_2]^{3-}$ Cluster in apo-ORP*. The metal cluster, $[Ag^{I}(MoS_4)_2]^{3-}$, is reconstituted in the recombinant protein employing a procedure similar to that described for Mo/Cu.[4] First, 1 mM $AgNO_3$ was added into 1 mM apo-ORP*, in 50 mM HEPES, pH 7.5, followed by the addition of 2 mM $(NH_4)_2MoS_4$; the mixture was incubated for 30 min in an ice bath (4 °C). The protein was subsequently separated from unbounded, small molecules (metal ions and TTM) by size-exclusion chromatography (PD-10 column; size exclusion of 5 kDa; GE Healthcare) equilibrated with 50 mM

DOI: 10.1021/acs.inorgchem.7b00840
Inorg. Chem. 2017, 56, 8900−8911

HEPES, pH 7.5, and the elution was carried out with the same buffer. The fraction containing the protein was collected and concentrated by ultrafiltration (centrifugation) using a YM5 membrane filter (size exclusion of 5 kDa; Sartorius).

2.5. Metal and Protein Quantification. The metals (silver, copper, and molybdenum) contents of Mo/Ag-ORP* and Mo/Cu-ORP* derivatives were determined by inductively coupled plasma (ICP) emission analysis in a Jobin Yvon Ultima instrument using the Re-agecom 23 ICP multi-elements as a standard solution over a concentration range of 0.05−6 ppm. The protein concentration was determined by the Lowry method,[36] using bovine serum albumin (BSA) as a standard protein. ICP: (Mo/Ag-ORP*) Mo:Ag = 1.98:1 (Mo:Ag:ORP* = 1.85:0.92:1) and (Mo/Cu-ORP*)[6] Mo:Cu = 1.90:1 (Mo:Cu:ORP* = 1.96:0.96:1).

2.6. Spectroscopic Studies. *2.6.1. UV−Visible.* UV−visible absorption spectra were collected using a Shimadzu UV-1800 spectrometer.

2.6.2. NMR. a. Sample Preparation. Fusion protein buffer was exchanged for 50 mM Tris-HCl buffer, pH 7.6, 10 mM phosphate buffer, pH 7.6, or 20 mM HEPES buffer, pH 7.5, prior to spectra acquisition by dialysis over a 3.5 kDa cutoff membrane. Protein samples were then concentrated to 0.6−1.5 mM using a Vivaspin centrifugal concentrator with a 5 kDa cutoff membrane. All samples contained D_2O (10%, v/v; Eurisotop). For the acquisition of metal-coordinated ORP* spectra, aliquots of 100 mM $CuCl_2$ were added to the sample in relevant ratios before spectra acquisition in 50 mM Tris-HCl, pH 7.6. In some spectra, DTT and TTM were also added in relevant concentrations. The apo-ORP* (1.2 mM) in 20 mM HEPES, pH 7.5, was titrated with 0, 20, 40, 60, 80, and 100% of $AgNO_3$.

b. ^1H NMR. All spectra were acquired at 298 K on a Bruker Avance III Ultrashield 600 MHz spectrometer equipped with a TCI cryoprobe and a variable-temperature control unit. The pulse sequence used in these experiments—zgesgp—contains a water suppression sequence based on excitation sculpting and gradient pulses. The spectral window was centered on the water resonance over 29 761 Hz (50 ppm), with a resolution of 128k points. Spectra were calibrated on the basis of the position of the water resonance. A total of 128 transients were accumulated per scan. Processing was performed using TOPSPIN 3.2 (Bruker).

c. 2D NMR. Spectra were acquired using ^{15}N at natural abundance samples at 298 K on a Bruker Avance III Ultrashield 600 MHz spectrometer equipped with a TCI cryoprobe and a variable-temperature control unit. ^{15}N,^1H-HSQC spectra were obtained by using a phase-sensitive and water flip-back pulse sequence (hsqcetfpf3gpsi2). The spectral widths were 12 019 Hz for ^1H and 3226 Hz for ^{15}N. A total of 2048 data points in t2 transients for each of the 128 t1 points were used, and 400 scans were collected per sample. NMR spectra were processed with TOPSPIN 3.2 provided by Bruker and analyzed with CARA 1.8.4.[37] Chemical shift perturbation for each amide resonance, $\Delta\delta_{HN}$ (ppm), was calculated as a combination of the changes in the proton ($\Delta\delta_H$) and nitrogen ($\Delta\delta_N$) dimensions according to the following equation:[38]

$$\Delta\delta_{HN} = \sqrt{\frac{\Delta\delta^2{}_H + (\Delta\delta^2{}_N/5)}{2}}$$

2.6.3. EPR. The apo-ORP* (1.5 mM) was titrated with 0.3, 0.6, 1, 2, 3, and 4 equiv of $CuCl_2$, in 50 mM Tris-HCl, pH 7.6, and the formation of Cu^{II}-ORP* was followed by EPR spectroscopy. The EPR spectrum of 1.5 mM $CuCl_2$ (in the same Tris-HCl buffer) was also acquired to guarantee that the spectra observed in the presence of apo-ORP* are in fact due to the formation of a Cu^{II}-ORP* complex. The Cu^{II}-ORP* formation was also studied in 50 mM phosphate buffer, pH 7.6. The spectra obtained in both buffers are identical, indicating that buffer does not interfere in the complex formation at pH 7.6. To follow the subsequent formation of the native Mo/Cu cluster, 2 equiv of TTM was added to one sample of Cu^{II}:ORP* 1:1, followed by the addition of 10 equiv of DTT. The spectra were acquired at 10−100 K, and no significant differences were found. The X-band EPR (9.65 GHz) spectra of all samples were recorded using a Bruker EMX 6/1 spectrometer and a dual-mode ER4116DM rectangular cavity (Bruker); the samples were cooled with liquid helium in an Oxford Instruments ESR900 continuous-flow cryostat, fitted with a temperature controller. The spectra were acquired at different temperatures (as indicated) and with a modulation frequency of 100 kHz, modulation amplitude of 0.1−0.5 mT, and microwave power of 0.633−2.01 mW.

2.7. Monomer−Dimer Determination. Molecular weight of protein samples (apo-ORP* and Cu^{II}-ORP*) is determined by gel filtration, comparing an elution volume between protein sample (apo-ORP* and Cu^{II}-ORP*) and standard samples. GE Healthcare Calibration Kits provide highly purified, well-characterized, globular protein standards (Apr, aprotinin (6500 Da); R, ribonuclease A (13 700 Da); CA, carbonic anhydrase (29 000 Da); C, conalbumin (75 000 Da)) for protein molecular weight determination, and a Superdex-75 10/300 GL column was used for this purpose. The column was washed and run with 50 mM Tris-HCl, pH 7.6, with 50 mM NaCl. The concentrations of apo-ORP* and Cu^{II}-ORP* all are 150−200 μM, and the mix standard protein solution is 3 mg/mL.

2.8. *In Silico* Docking. The HADDOCK algorithm[39] was used to calculate likely binding poses between two different ORP monomers. HADDOCK was accessed via the WeNMR portal.[40] The structure of *D. gigas* apo-ORP* was downloaded from the Protein Data Bank (PDB file 2WFB) and prepared for the procedure using UCSF Chimera's[41] Dock Prep tool. The single ambiguous interaction restraints used for HADDOCK determined that H_{53} from one polypeptide chain had to be in the vicinity of H_3 from the other chain. Interaction interfaces were evaluated using the binding affinity algorithm PRODIGY.[42]

3. RESULTS AND DISCUSSION

3.1. Synthesis. The ATCUN tag-containing *D. gigas* apo-ORP* was overexpressed and purified without the Mo/Cu cluster, as previously described.[34]

Upon addition of $CuCl_2$ into apo-ORP*, the Cu^{II} interacts with a particular region (ATCUN) of the ORP* sequence directly, and failed to continue the further process of cluster formation in the presence of TTM, in spite of TTM's extraordinary affinity toward copper and reducing ability. To overcome this problem, we first added TTM into the apo-ORP*, and only after this step, $CuCl_2$ was added to this mixture, to form a different cluster—Cu^I-TTM—as judged by its UV−visible spectrum.[5,6] The Mo/Cu cluster is formed only when the Cu^{II} ion in the Cu^{II}-ORP* complex is reduced to Cu^I and subsequently binds TTM in the presence of DTT. Therefore, it can be anticipated that, during cluster assembly, copper enters in the Cu^I oxidation state in apo-ORP (*in vivo*), and then TTM binds Cu^I in the cluster-binding region. From this observation, we became highly interested in the study of the binding site of Cu^{II} using UV−visible, NMR, and EPR spectroscopies. Ag^I is used as a probe of Cu^I to support the Cu^I-binding site by ^1H NMR spectroscopic studies.

3.2. Absorption Spectroscopy of ORP* in the Presence of Added Metals. *3.2.1. Copper.* We first focused on copper-coordination chemistry after addition of $CuCl_2$ into apo-ORP*. Cu^{II} binding was monitored by visible electronic absorption spectroscopy upon titrating of apo-ORP* with increasing amounts of Cu^{II}. At stoichiometric Cu^{II}:ORP* ratios, a single visible electronic absorption band appeared at 520 nm ($\varepsilon \approx 90\ M^{-1}\ cm^{-1}$), saturating at one equivalent, typical of a Cu^{II} d−d transition (Figure 2) (pH range 7.0−8.0). Deprotonation of amide nitrogen in aqueous medium ion requires strongly basic conditions ($pK_a \approx 15$) in the absence of metal. But the process is significantly enhanced in the presence of Cu^{II} when the imidazole ring of the histidine residue is available to act as an anchor for the metal ion.[43−45] An excess of

DOI: 10.1021/acs.inorgchem.7b00840
Inorg. Chem. 2017, 56, 8900−8911

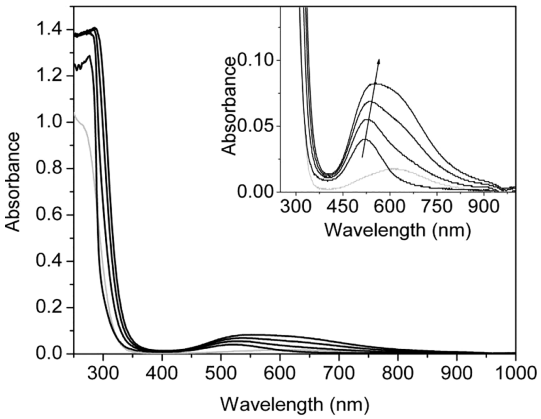

Figure 2. UV−visible spectra of apo-ORP* (~400 μM) with $CuCl_2$ (black lines, 400, 800, 1200, and 1600 μM $CuCl_2$) and 400 μM $CuCl_2$ (alone) in 50 mM Tris-HCl buffer, pH 7.6 (gray line). Inset: enlargement to show the peak intensity of the d−d transition.

Cu^{II} relative to apo-ORP* leads to a band shift toward higher wavelengths, with a change in color from purple to blue (618 nm) indicative of excess free $CuCl_2$. Upon removal of excess $CuCl_2$ (PD-10 desalting column), it returns to the purple color. The peak at 520 nm with low molar absorptivity ($\varepsilon \approx 90$ M^{-1} cm^{-1}) is in agreement with a d−d transition of a coordinated Cu^{II} ion, probably due to 4N-donor set of peptide sequence/motif of ORP*. A vast body of literature supports the assignment of coordination modes of these spectroscopic species as those with four nitrogen atoms coordinated equatorially to the Cu^{II} ion. Peptides with histidine residue in the third position from the amino-*N*-terminus display absorbance at 520 nm characteristic of a typical Cu^{II}-ATCUN-binding site.[46]

The Mo/Cu cluster formation is shown in Figure 3. The stable Cu^{II}-ATCUN complex cannot bind TTM. However,

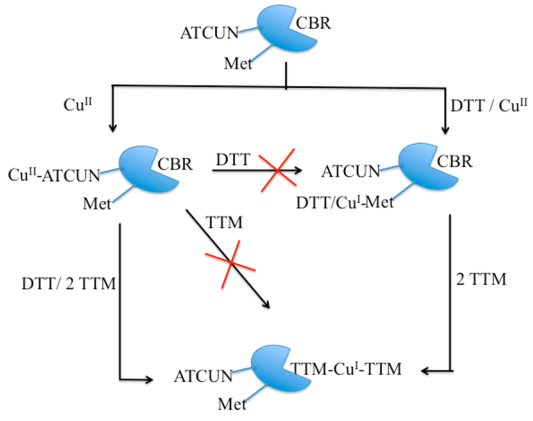

Figure 3. Chemically synthesis of Mo/Cu cluster in ORP* (CBR, cluster-binding region).

when TTM is added into Cu^{II}-ORP* solution in the presence of DTT, the peaks at 469 and 317 nm (free TTM) slowly shifted to 480 nm ($\varepsilon = 7850 \pm 500$ M^{-1} cm^{-1}) and 340 nm ($\varepsilon = 11\,800 \pm 750$ M^{-1} cm^{-1}) respectively, an indication of the formation of $[Cu^{I}(MoS_4)_2]^{3-}$ cofactor, which is monitored by UV−visible spectra over 2 h at RT (Figure 4A). DTT reduces Cu^{II}-ORP* to Cu^{I}-ORP*, which can bind TTM to form the metal cofactor, but neither TTM nor DTT alone can reduce Cu^{II} to Cu^{I}. The DTT (2- to 10-fold excess)-dependent reduction of Cu^{II}-ORP* was tested under anaerobic conditions, with the copper reduction being monitored by a decrease of the Cu^{II}-ORP* signal at 520 nm. The intensity of this peak remains unchanged over a period of 2 h, indicating an inability of DTT to reduce copper. Upon addition of TTM into this solution (Cu^{II}-ORP* + DTT), the Cu^{II} is reduced to Cu^{I}, and clusters form even under aerobic conditions. Here TTM acts as a Cu^{I}-chelator with strong affinity, which enforced to reduction in the presence of DTT (Figure 3A) to cluster formation. When DTT (2-fold excess) was first added into apo-ORP* followed by the Cu^{II} salt, no Cu^{II}-ATCUN signal was observed at ~520 nm under anoxic conditions. Under reducing environment (DTT), addition of Cu^{II} leads to its reduction to Cu^{I}, which is unable to bind the ATCUN site and immediately yields $[Cu^{I}(MoS_4)_2]^{3-}$ in the ORP pocket in the presence of TTM (2-fold) (Figure 4B). Cu^{I} may be binding the thiol groups of DTT molecules since thio-ether is a weaker coordinating ligand than thiol. However, as described in the literature, ATCUN favors only Cu^{II} binding over Cu^{I}.[21−23] So, the coordination mode of Cu^{II} in this system now understood but the coordination site at Cu^{I} remains elusive. Under physiological conditions, copper preferably binds histidine, cysteine and/or methionine side chains, based on the oxidation state of copper. Since Cu^{II} preferably binds histidine and is well known to bind the ATCUN site, Cu^{I} may bind a soft sulfur site,[21−23] methionine (as cysteine is absent), which is close to the ATCUN site (see crystal structure; Figure 1B).

3.2.2. Silver. The solubility of Cu^{I} in aqueous buffer, as well as stability/folding of ORP in organic solvent (%), is problematic. To overcome these limitations, silver (Ag^{I}) was used as a surrogate probe of Cu^{I}, since Cu^{I} and Ag^{I} ions exhibit similar charge and behavior.[47,48] The $[Ag^{I}(MoS_4)_2]^{3-}$ cluster is synthesized in apo-ORP* in the presence of $AgNO_3$ and TTM, as shown by UV−visible spectrum (Figure S1). The UV−visible spectrum shows two characteristic bands at 322 nm ($\varepsilon = 13\,600 \pm 700$ M^{-1} cm^{-1}) and 475 nm ($\varepsilon = 8550 \pm 400$ M^{-1} cm^{-1}) which are ascribed to the $[Ag^{I}(MoS_4)_2]^{3-}$ cluster.[49,50] Therefore, Ag^{I} does not bind the ATCUN site and may actually bind at the methionine site first. This hypothesis is supported by the NMR study (see below). It has been also shown both *in vivo* and *in vitro* that Ag^{I} can replace Cu^{I} in its native binding sites in copper proteins.[51,52]

3.3. ^{1}H NMR Spectroscopy of ORP* in the Presence of Added Metals. *3.3.1. Copper.* The slow electron spin relaxation of paramagnetic Cu^{II} ions causes broadening of proton NMR resonances linked to paramagnetic centers through-bond (contact) or through-space (pseudocontact) interactions.[53,54] 1D (^{1}H) NMR experiments were carried out analyzing the amide, the aromatic, and the aliphatic regions of the NMR spectra of apo-ORP* and apo-ORP* titrated with $CuCl_2$ at pH 7.6 in 50 mM Tris-HCl buffer and used to assign the signals of the key amino acids residues. The addition of $CuCl_2$ (0−70%) into a tube containing apo-ORP* (1.5 mM) caused selective broadening of resonances, which provided an indication of the location of copper binding in ORP* as shown in Figure 5. Specific NMR signal alterations were observed through out the $CuCl_2$ titration experiments, suggesting that the metal ions selectively interact with the His_3 and His_{53} (Figure 5). In the aromatic region, the spectrum is significantly affected in the following regions: 7.66−7.60 ppm (7.634 (a) and 7.617 ppm (b)) and 6.95−6.85 ppm (6.903 (d) and 6.889 ppm (e)). Histidine aromatic ^{1}H peaks usually appear as two singlets between 6.5 and 8.5 ppm.[55,56] The 7.66−7.60 and

DOI: 10.1021/acs.inorgchem.7b00840
Inorg. Chem. 2017, 56, 8900−8911

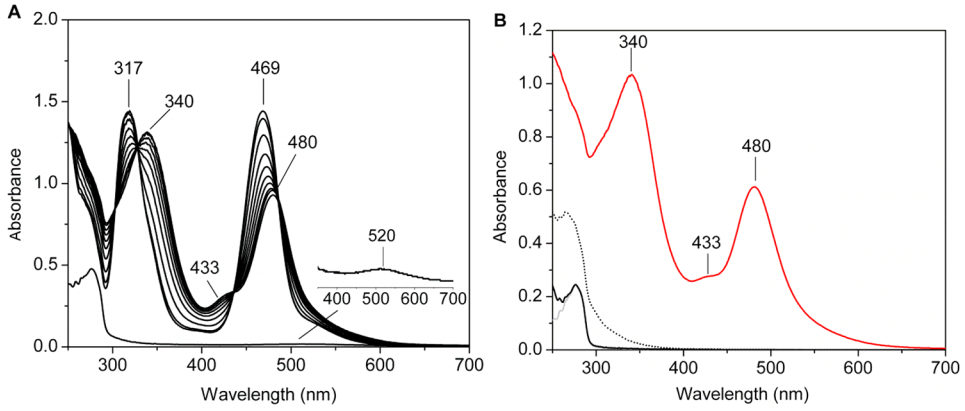

Figure 4. (A) UV−visible spectra of apo-ORP* (100 μM) with 100 μM $CuCl_2$ (lower trace, single; inset shows magnification at ∼520 nm region) and added 200 μM $(NH_4)_2MoS_4$ in the presence of 2 mM DTT in 50 mM Tris-HCl, pH 7.6, over 2 h every 15 min at RT. (B) UV−visible spectra of apo-ORP* (75 μM) (gray) with 1 mM DTT (black) and after addition 75 μM $CuCl_2$ (dotted) and 150 μM $(NH_4)_2MoS_4$ (red) in 50 mM Tris-HCl, pH 7.6, over 5 min at RT.

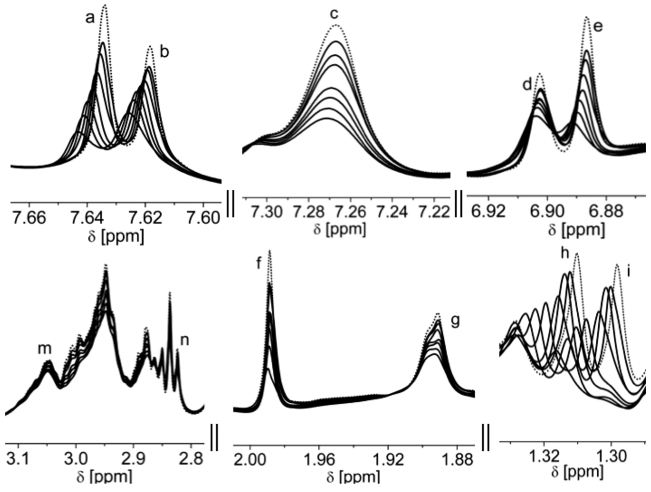

Figure 5. ^{1}H NMR (600 MHz) spectra of apo-ORP* (1.5 mM) (dotted black) and apo-ORP* (1.5 mM) titrated with $CuCl_2$ (0−70%)] (black) in 50 mM Tris-HCl at pH 7.6/D_2O (80/20%). The only regions represented and expanded are those are highly affected by paramagnetic Cu^{II}, labeled as a, b; c; d, e; m−n; f, g; and h and i peaks.

6.95−6.85 ppm regions are assigned to H_ε and H_δ protons of two histidine residues, His_3 (H_ε = 'a' and H_δ = 'e') and His_{53} (H_ε = 'b' and H_δ = 'd'), respectively according to previous NMR data of ORP*.[34,57] In presence of 70% $CuCl_2$, peaks 'a' and 'b' suffer a downfield chemical shift to 7.641 and 7.624 ppm, respectively, with peak 'a' being more affected compared with peak 'b'. Peaks at 6.886 (e) and 6.902 ppm (d) suffer the same fate, shifting to 6.889 (e) and 6.903 ppm (d), respectively; likewise, the intensity of peak 'e' is more affected than that of peak 'd'. This result indicates that one histidine (His_3) directly interacts with Cu^{II} while the other histidine (His_{53}) suffers the pseudo-contact effects of paramagnetic Cu^{II} ions. Thus, Cu^{II} binds tightly at His_3 site in *N*-terminus. This result is also comparable with copper binding to other ATCUN containing peptide/proteins.[55,56] The peak at 7.267 ppm (c) is also affected; this peak may be ascribed to a glutamine (Q_{61}) or arginine (R_6) side chain. At alkaline pH, the amide resonances were in fast exchange with the solvent and could not be observed in the NMR spectrum.

Peaks in the aliphatic region of the ^{1}H NMR spectrum were also affected, namely those at 3.05−2.8 (m−n), 1.987 (f), 1.890 (g), 1.310 (h), and 1.298 ppm (i). The resonance peaks at 'h' and 'i' are broadening and chemically shift downfield to 1.325 and 1.313 ppm, respectively; they likely belong to the methyl group (doublet peaks) of alanine (A_1),[34,57] the *N*-terminus amino acid. Multiple resonances at 3.1−2.8 ppm, assigned to the histidine β-protons, and a singlet peak at 1.987 ppm may be assigned to the -S-CH_3 of methionine whose intensity also significantly decreased. This peak assignment is confirmed by addition of H_2O_2 into apo-ORP*, where only this particular peak is highly affected. The peak at 1.987 ppm (f) decreased while a resonance peak at 2.623 ppm appeared and saw its intensity rise,[58,59] which indicated the formation of oxidized methionine peak, (−S(O)−CH_3) (Figure S2).

^{1}H NMR was employed to gain insights into the precise location of cofactor binding in ORP. Upon titration of Cu^{II}-ORP* with TTM (2 equiv), the overall spectrum is affected

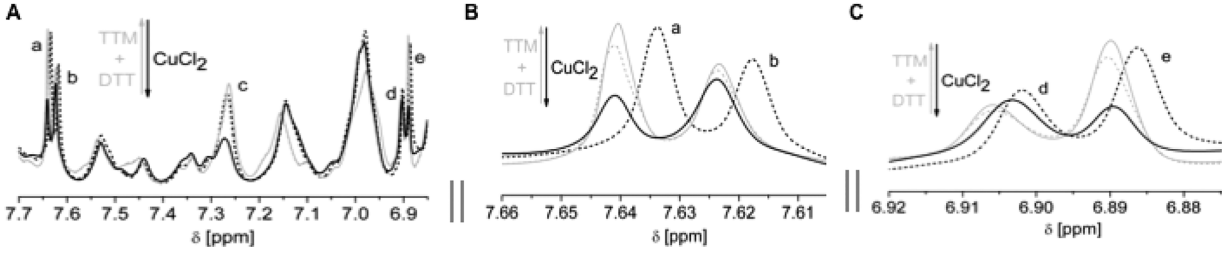

Figure 6. (A) ^{1}H NMR (600 MHz) in the aromatic region (7.7−6.8 ppm) of apo-ORP* (1.5 mM) (dotted black) in 50 mM Tris-HCl at pH 7.6/D_2O (80/20%) with 50% $CuCl_2$ (black), 100% of TTM, and DTT (10 mM) over 1 h (dotted gray) and 2 h (gray). 'a', 'b', 'c', 'd', and 'e' represented highly affected peaks. (B) Magnification of the a and b peaks. (C) Magnification of the d and e peaks. Arrows indicate the direction.

DOI: 10.1021/acs.inorgchem.7b00840
Inorg. Chem. 2017, 56, 8900−8911

(not shown), likely as a result of TTM adsorbing onto the protein surface. The addition of a 10-fold excess (10 mM) of DTT sees the particular peaks (a, b, c, d, and e), which are highly affected by Cu^{II}, return to their initial intensity (Figure 6). The proposed histidine resonance site intensity increased, meaning that the Cu^{II} reduced to Cu^{I} in the presence of DTT and subsequently binds TTM to form the ORP cofactor; the Cu^{I} cannot bind histidine residue directly anymore. In the presence of 50% $CuCl_2$ in 1.5 mM apo-ORP*, the five resonances in the aromatic region, 'a', 'b', 'c', 'd', and 'e' suffered considerable broadening and shifted to 7.641, 7.624, 7.270, 6.889, and 6.903 ppm, respectively. In the presence of 100% TTM and 10-fold excess of DTT (10 mM), the 'a', 'b', 'c', 'd', and 'e' peaks return almost to their initial intensity (Figure 6). This result indicates the formation of the metal cofactor in ORP in this region. The un-coordinated histidine side chain may interact with sulfur atoms of the metal cofactor by H-bonding to stabilize, resulting in a resonance shift. Figure 6 (cluster formation) shows that the particular 'd' peak is shifted toward higher ppm while its intensity decreases. This result indicates that the Nε atom of the His_{53} imidazole side chain is specifically hydrogen bonded to a bridging sulfur atom. This interaction is also found in nitrogenase, where the structure of nitrogenase revealed that the α-His_{195} residue provides one of three NH−S hydrogen-bonding interactions with one of the bridging S atoms of the FeMo cofactor.[60]

Since the protein binds the anionic cluster via non-covalent interactions, phosphate anions (in the buffer) were introduced as competitors with the metal cofactor for protein binding. The apo-ORP* in 50 mM Tris-HCl was dialyzed overnight at 4 °C in 10 mM phosphate buffer, pH 7.6. The ^{1}H NMR spectrum is considerably different at the histidine site (Figure 7). In

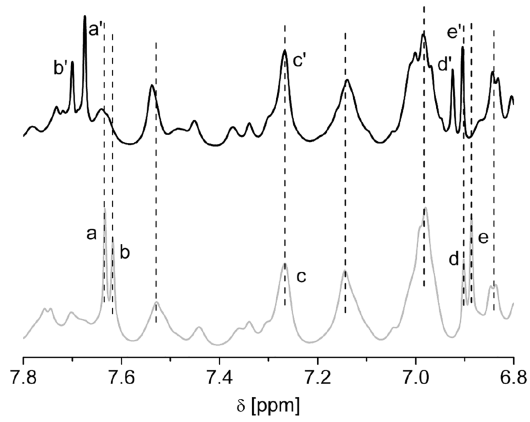

Figure 7. ^{1}H NMR (600 MHz) in aromatic region (7.8−6.8 ppm) of apo-ORP* in 50 mM Tris-HCl, pH 7.6/D_2O (80/20%) (gray, 1.5 mM), and 10 mM phosphate, pH 7.6/D_2O (80/20%) (black, 600 μM).

phosphate buffer, the main resonances are found at a′ = 7.701 (a = 7.635), b′ = 7.676 (b = 7.617), d′ = 6.925 (d = 6.904), and e′ = 6.905 ppm (e = 6.886). The main difference between two buffer systems is that the two resonances 'a' and 'b' exchanged peak positions with one another. These findings support the hypothesis that phosphate interacts with histidine-NH through hydrogen bonding to modify the configuration/orientation of histidine side chain. Upon adding $CuCl_2$ into apo-ORP* in phosphate buffer, the UV−visible spectrum displays a d−d band at 520 nm ($\varepsilon \approx 90$ M^{-1} cm^{-1}) which is similar to Cu^{II}-ORP* in Tris-HCl buffer (not shown). It means that the Cu^{II}-ligation site (4-N) remains same. Cu^{II} can strongly bind His_3 yielding other non-covalent interactions in the direction of the Cu^{II}−N coordination bond; as a result, the UV−visible (not shown) and EPR spectra (Figure S3) are the same in both buffers. Furthermore, Cu^{II} is more stable in amine buffer than in phosphate buffer, resulting in Cu^{II} being more affected in phosphate buffer.

3.3.2. Silver. An analogous behavior was observed when a silver salt ($AgNO_3$) was used instead of Cu^{I} in the interaction studies with thio-ether of model peptides/proteins.[47,48] The titration ^{1}H NMR spectra (Figure S4) of apo-ORP* with Ag^{I} displayed dramatic downfield shifts of Hε (-S-CH_3) resonances of methionine residues, indicating a specific binding of Ag^{I} to the methionine site, in accordance with the other methionine-rich peptide/proteins.[47,48] This result supports coordination between thioether (side chain of methionine) and Cu^{I} (or the Ag^{I} probe), with no affinity for divalent metal ions.

3.3.3. ^{15}N,^{1}H-HSQC Spectra of apo-ORP and Cu^{II}-ORP*.* The ^{15}N,^{1}H-heteronuclear single quantum coherence spectra (HSQC) of $CuCl_2$ incubated apo-ORP* showed the affected region (Figure 8). Backbone and side-chain chemical shift assignments were obtained in the *N*-terminus region, as well as some residues in the cluster-binding region. A wide range of amide protons, including the *N*-terminus Ala_1, Ser_2, Met_4, His_3, and His_{53}, were missing in the ^{15}N,^{1}H-HSQC spectrum of apo-ORP* because of fast exchange with a bulk solvent.[61,62] In the presence of $CuCl_2$, chemical shift changes were found to be significantly higher for residue 26 from the *N*-terminus site (His_3) and residues 26 (R_{26}), which, in the three-dimensional structure, are located near the cluster-binding site (His_{53}) (see Figure 10). These data suggest that residues from both the ATCUN site and the cluster-binding site of ORP* are involved in the interaction between two ORP* molecules. Comparison of the assignments obtained for apo-ORP* with Cu^{II}-ORP* revealed that most chemical shift perturbations also map (Figure 8) close to the metal-binding site, which are supported by our previous NMR spectroscopic analysis of the reconstituted holo-ORP from *D. alaskensis G20*[4] and *D. gigas*[5] in that the cluster-binding region includes a set of conserved residues D_{21}PRFGRA_{27}, H_{53}GAGIN_{58}, and L_{72}TGYVGPKAF_{81}.

3.4. EPR Spectroscopy of ORP* in the Presence of Added Metals. *3.4.1. Copper.* The apo-ORP* was titrated with $CuCl_2$ to determine the number of copper ions bound per ORP* molecule and to obtain independent information about the coordination sphere of the copper ion in Cu^{II}-ORP*. In the presence of 0.3, 0.6, and 1 equiv of Cu^{II} (Figure 9A, orange, red, and dark red lines, respectively), ORP* gives rise to a single S = 1/2 signal, characteristic of a Cu^{II} complex in a square-planar geometry (or square-planar with weak axial ligand(s)), with $g_{\|,\perp}$ = 2.183, 2.042 and $A^{Cu}_{\|,\perp}$ = 207 × 10^{-4} cm^{-1}, 19 × 10^{-4} cm^{-1}, hereafter designated "signal a" (simulated in black line of Figure 9A). This signal is clearly distinct from the one originated from $CuCl_2$ alone ($g_{\|}$ = 2.232, $A^{Cu}_{\|}$ = 198 × 10^{-4} cm^{-1}; Figure 9A, gray line), thus demonstrating that it arises from a Cu^{II}-ORP* complex. A plot of the signal intensity (double integration of the EPR spectra) versus the amount of copper added demonstrates that "signal a" arises from a 1:1 Cu:ORP* complex (Figure 9B).

Further addition of 2, 3, and 4 equiv of Cu^{II} to apo-ORP* (Figure 9A, light blue, blue, and dark blue lines, respectively) leads to the emergence of other signals that eventually dominate the spectrum, hereafter designated as "signals b"

DOI: 10.1021/acs.inorgchem.7b00840
Inorg. Chem. 2017, 56, 8900−8911

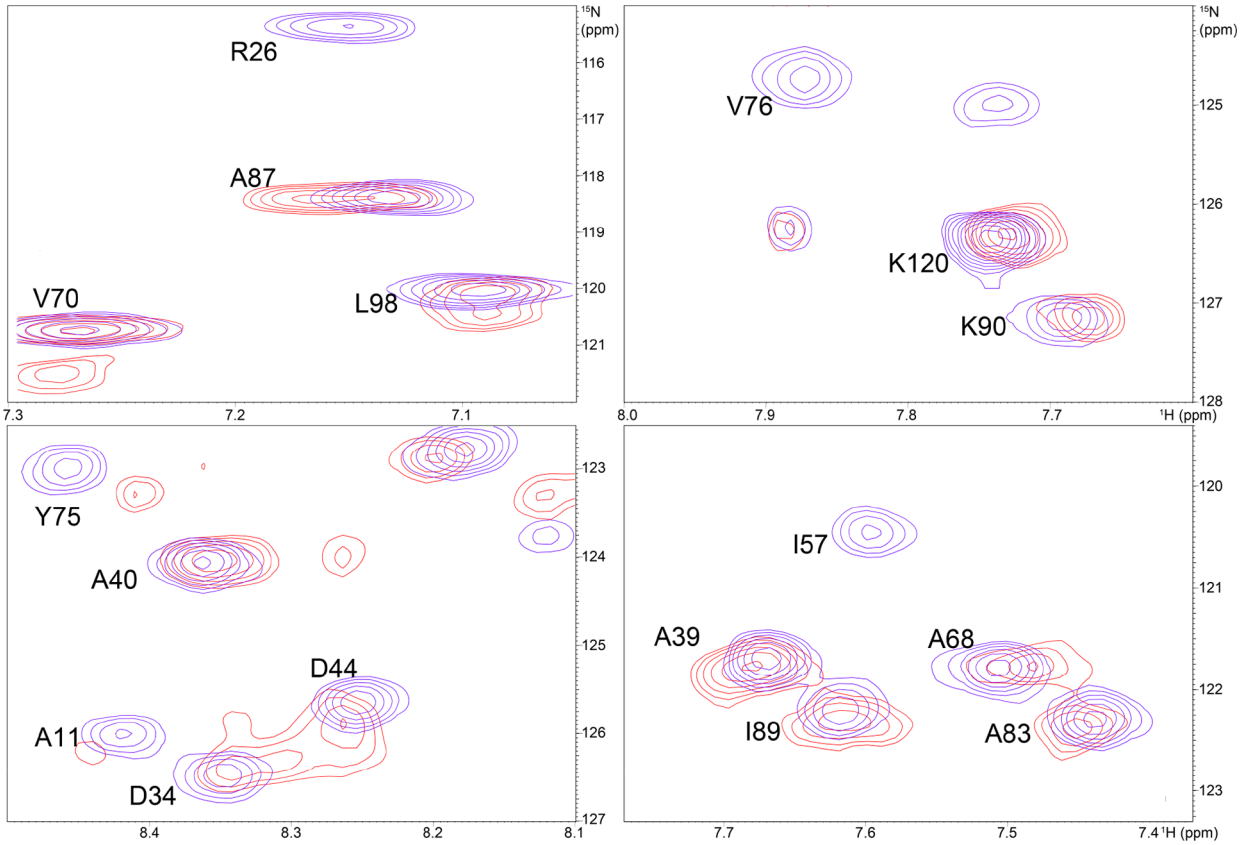

Figure 8. ^{15}N,^{1}H-HSQC spectra of Cu^{II}-ORP* (red) compared with apo-ORP* (blue), showing some of the most affected residues, including R_{26} (broadened beyond detection), Y_{75} (largely shifted), and V_{76} (broadened beyond detection) in the copper variant in 50 mM Tris-HCl, pH 7.6, at RT.

($A^{Cu}_{||}$ features indicated by blue arrows in Figure 9A). Because "signals b" are also distinct from the one of $CuCl_2$ alone, they must arise from copper bound to ORP*. Yet, "signal a" and "signals b" originate from Cu^{II} ions bound to different sites of ORP* (different compositions and/or geometries), as evidenced by their different $g_{||}$ and $A^{Cu}_{||}$ values. The significant absence of the signal from $CuCl_2$ alone in the Cu:ORP* 4:1 spectrum shows that the 4 equiv of copper is bound to ORP* (~91% according to Figure 9B) and that "free", "aquoso" copper is negligible. Therefore, ORP* is able to bind at least ~4 equiv of copper through both the ATCUN motif and other sites.

The "Truth Diagram" derived originally by Peisach and Blumberg can give insights into the type of ligands involved in the copper coordination.[63] The "signal a" $g_{||}$ and $A^{Cu}_{||}$ values (2.183 and 207 × 10^{-4} cm^{-1}) are typical of both a four-nitrogen coordination site and a two-nitrogen and two-oxygen coordination site. However, only a four-nitrogen coordination site is also supported by the UV−visible data (a d−d transition band at 520 nm; ε = 90 M^{-1} cm^{-1}).

The wavelength of the maximum visible absorption can be used as an indication of the number of nitrogen ligands of a Cu^{II} complex,[64] with a increasing number of nitrogen ligands causing a decrease in the wavelength of the maximum visible absorption (765 nm for one nitrogen, to 540 nm for four nitrogen ligands).[65] Moreover, "signal a" displays partially resolved nitrogen super-hyperfine interaction(s) in the $g_{\perp}$ region (325−335 mT) (Figure 9A, orange, red, and dark red lines), even though it is impossible to determine the number of nitrogen atoms involved.

The "signal a" is remarkably similar to other signals originated from proteins and small peptides known to bind copper through an ATCUN motif.[66−68] As in those proteins, it is highly probable that ORP* coordinates one Cu^{II} ion in a tetradentate mode by one histidine imidazole nitrogen, one *N*-terminus amine, and two deprotonated amide nitrogen atoms.

To follow the formation of the native Mo/Cu cluster, one sample of Cu:ORP* 1:1 was treated with 2 equiv of TTM. Yet, the spectrum of the Mo:Cu:ORP* 2:1:1 sample is indistinguishable from that of the Cu:ORP* 1:1 sample. After the addition of 10 equiv of DTT, the spectrum intensity begins to decrease with time; after 2 h, the spectrum is completely abolished (not shown), thus showing that Cu^{II} was totally reduced to Cu^{I} and suggesting that the native Mo/Cu cluster was formed, in accordance with the NMR and UV−visible data described above.

3.5. Probable Structure, Protein−Protein Interaction, and Cluster Formation Mechanism. The spectroscopic data gathered reveal only one metal-binding site at the *N*-terminus ATCUN-binding motif[26] coordinating in a square planar geometry by the *N*-terminus amine, the imidazole, and the two amide nitrogens in between (Figure 10). ^{1}H NMR clearly indicates that two histidines (His_3 from the ATCUN motif and native His_{53}) are highly affected—the former more than the latter. This implies that His_3 is directly bound to the metal center while His_{53} is affected by the paramagnetic effect; however, their relatively large distance ($d_{C\alpha\text{-}C\alpha}$ = 27.9 Å) precludes any metal-induced, long-distance paramagnetic effect. We propose herein an intermolecular protein−protein interaction to explain the observed effect. The *N*-terminus

DOI: 10.1021/acs.inorgchem.7b00840
Inorg. Chem. 2017, 56, 8900−8911

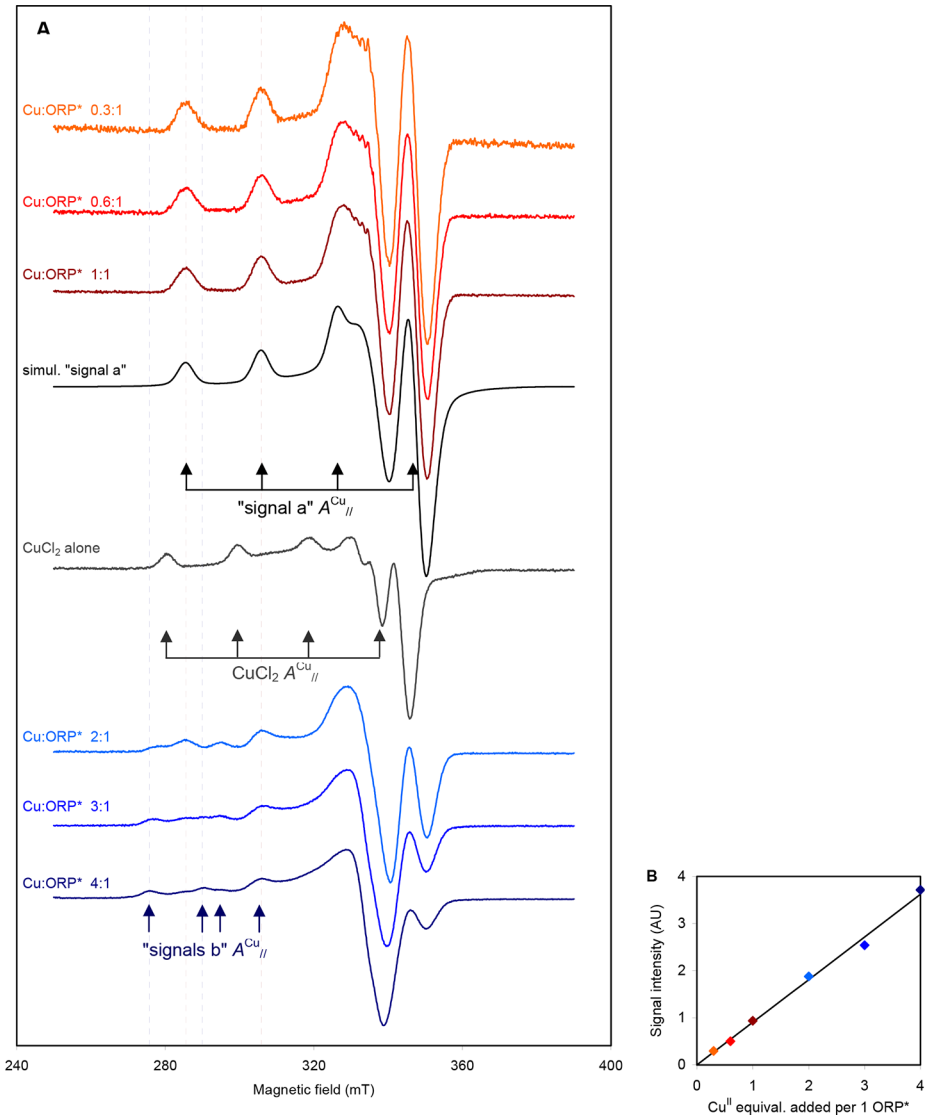

Figure 9. Titration of apo-ORP* with 0.3, 0.6, 1, 2, 3, and 4 equiv of $CuCl_2$ followed by EPR spectroscopy at 40 K (orange, red, dark red, light blue, blue, and dark blue lines, respectively). (A) The EPR spectra were multiplied by different factors to facilitate the comparison (the spectra obtained with 0.3, 0.6, 1, 2, 3, and 4 equiv of Cu^{II} were multiplied by 3, 3/2, 1, 1/2, 1/3, and 1/4, respectively). The spectrum of $CuCl_2$ alone is also presented (gray line). Simulation of the signal obtained with 1 equiv of Cu^{II}, herein designated "signal a", is presented as a black line. The main $A^{Cu}_{||}$ features are indicated by arrows. Samples were prepared and spectra acquired as described in the Materials and Methods. (B) The intensity of each spectrum (obtained by double integration of the EPR spectrum) was plotted against the amount of copper added per equivalent of ORP* (points are color-coded with the same colors used in the spectra). The intensity of the spectra was normalized considering that the spectrum of 1 equiv of $CuCl_2$ alone has an intensity of 1 (AU, arbitrary units). The line slope was 0.905 (r^2 = 0.995).

metal-binding ATCUN site interacts with the cluster-binding region in a head-to-tail fashion via non-covalent interactions, explaining the possibility of metal paramagnetic effects or H-bonding affecting these resonances (Figure 10). Protein−protein interactions are often found in biological systems contributing to several cellular pathways.[10]

Apo-ORP* and Cu^{II}-ORP* were subjected to analytical size exclusion column chromatography, the elution volume of the protein displays two peaks which confirm dimer (small trace) and monomer state of ORP* (Figure S5). The apo-ORP* and Cu^{II}-ORP* gave the same result. Such behavior is characteristic of a self-associating protein.[69]

The more polar, charged residues (Arg, Lys, Gly, Gln, His, etc.) in the interfaces of protein surface are the most likely candidates to mediate the specific interactions in these regions.[70] From the 10 analyzed clusters from HADDOCK[39] (Figure 11), each complex is stabilized on average by 5.9 ± 3.4 and 3.5 ± 2.9 interactions between the side chains of charged and apolar or polar and apolar amino acids, respectively. The overall K_d predicted for the 10 best complexes is 1.0 ± 0.8 mM in the absence of metal, supporting the metal-mediated formation of a dimer, as this value is characteristic of very weakly binding partners.

A proper cluster assembly is essential for protein function. The assembly and metalation of metalloenzymes is a complex process *in vivo*, requiring a large number of accessory proteins: CuA assembly,[71] Mo−Cu−CODH,[72] FeMoco-nitrogenase,[73] etc. Although Mo/Cu cluster formation in ORP *in vivo* is complex, we can put forward a proposal for the Mo/Cu cluster formation. The X-ray structure[35] of apo-ORP* also showed that all methionine residues are located in the ATCUN-His_3 side, which is opposite to the cluster-binding site His_{53} (Figure

DOI: 10.1021/acs.inorgchem.7b00840
Inorg. Chem. 2017, 56, 8900−8911

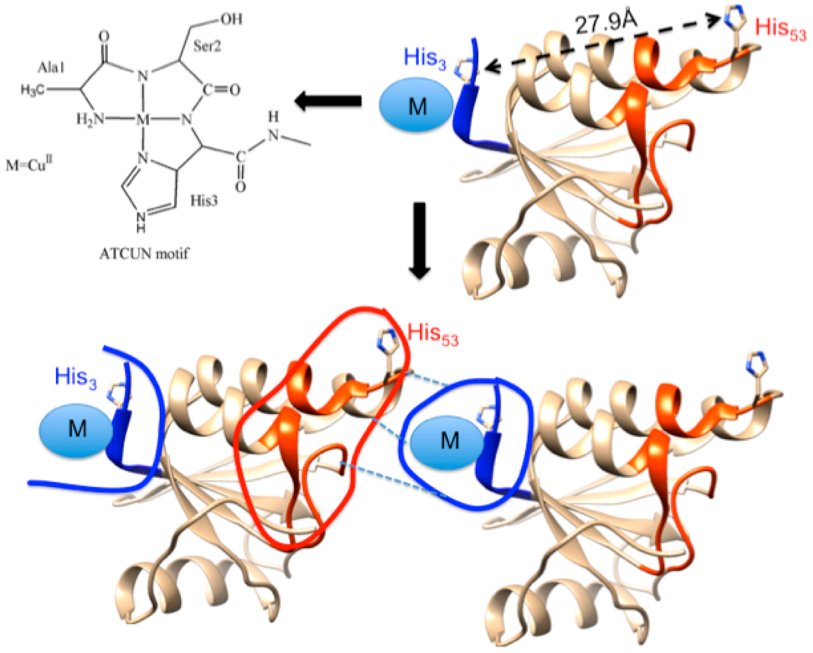

Figure 10. Schematic diagram of metal-binding ATCUN motif and protein−protein interaction between two M-ORP* molecules through noncovalent interaction (blue dotted lines). Two interfacing surfaces of two M-ORP* molecules are highlighted: M-ATCUN region ($A_1S_2H_3$) with $M_4G_5R_6$ residues (blue) and metal-binding region containing conserved residues D_{21}PRFGRA_{27}, H_{53}GAGIN_{58}, and L_{72}TGYVGPKAF_{81} (reddish-orange). Structures of apo-ORP* are deduced from PDB file 2WFB[35] and represent distances between two histidine(s).

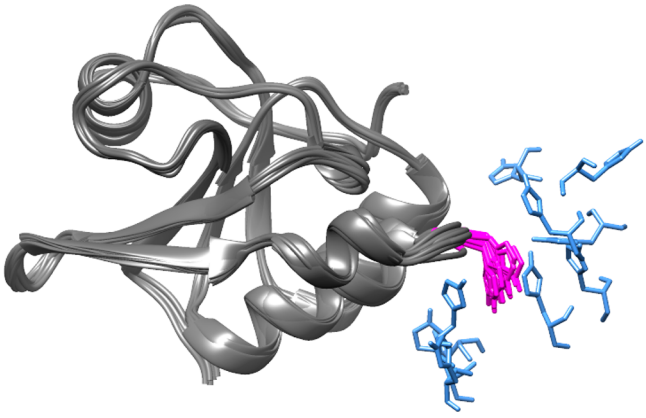

Figure 11. Proposed docking interactions predicted by HADDOCK.[39] Ten structures of ORP* are shown as superimposed dark gray ribbons, with interacting H_{53} in magenta. For clarity reasons, only His_3 of each of the 10 best interacting clusters is shown (light blue), with the rest of the protein omitted.

1B). In biological systems, copper is bound predominantly by the three main amino acid with different side chain chemical groups—imidazole, thiolate, and thioether—to optimize copper acquisition under different environmental conditions.[22,23] The thioether functional group provides a neutral sulfur donor that does not have the same pH dependence of histidine, is more hydrophobic than histidine, and generally prefers Cu^I rather than Cu^{II}. So cluster formation may be proposed as reduced Cu^I may be ligated by two methionine residues which are located in the vicinity of each other (Met_4 and Met_{114}; d_{S-S} = 7.025 Å), yielding an intermediate {Met_4-Cu^I-Met_{114}} structure that may interact with the cluster-binding site of another apo-ORP molecule. This distance can be fitted in Cu−$S_{thioether}$ bond distances (2.25−3.3 Å) in synthetic compounds as well as in copper-proteins.[74−76] Finally, in the presence of TTM, the {Met_4-Cu^I-Met_{114}} unit releases the Cu^I to bind with TTM to afford final metal cofactor.

Based on our results, we suggest that Cu^I does not bind in the same way that Cu^{II} does to the ATCUN site alone. This is not surprising because the soft Cu^I would disfavor the harder donor character of amide and amine nitrogen according to Pearson's HSAB principle.[77] The unique feature of methionine in ORP selectively binds Cu^I and transports it to the cluster-binding site by transient interactions between two proteins. The fusion amino acid, His_3, binds Cu^{II}, and the stable copper complex gives solid information about cluster assembly through protein−protein interactions—thanks to the ATCUN tag.

4. CONCLUSIONS

In this study, we have investigated the binding of Cu^{II} to the fusion ORP protein containing the ATCUN motif, ORP*. The EPR and UV−visible spectra clearly show that the ORP* binds Cu^{II} stoichiometrically, to form a 1:1 Cu^{II}-ORP* complex, where the copper ion is coordinated by four nitrogen atoms of the ATCUN motif. In the presence of higher amounts of copper, the emergence of different EPR signals suggests that ORP* is able to bind at least ∼4 equiv of copper, through both the ATCUN motif and other sites. NMR results extend the UV−visible and EPR results and clearly show that metal ions interact not only with the *N*-terminus ATCUN motif (His_3) but also with the cluster-binding site (His_{53}), which is very far away (His_3---His_{53}; $C_\alpha-C_\alpha \approx$ 27.9 Å), suggesting the intermolecular protein−protein interaction that is also supported by docking analysis. ^{1}H NMR of Ag^I-ORP* supports the coordination chemistry of Cu^I-thiother in a specific methionine site which may play an additional, copper-sensing role in the cluster formation pathway. In cluster assembly in ORP*, the probable mechanism is that Cu^{II} is first reduced to Cu^I, and then the coordination site changes from ATCUN to the thioether site to afford the {Met_4-Cu^I-Met_{114}} intermediate,

DOI: 10.1021/acs.inorgchem.7b00840
Inorg. Chem. 2017, 56, 8900−8911

which is directed toward the cluster-binding site of the other molecule through a non-covalent interaction, and finally TTM binds with Cu^{I} to afford native Mo/Cu-metal cofactor, releasing Cu^{I} from the methionine site. This model protein/peptide provides a new insight into copper recruitment/transport via intermolecular protein−protein interaction and is also relevant to copper trafficking pathways involving proteins, which transport copper ions into final target proteins in bacteria and eukaryotes.

■ ASSOCIATED CONTENT

Supporting Information

The Supporting Information is available free of charge on the ACS Publications website at DOI: 10.1021/acs.inorgchem.7b00840.

UV−visible spectra of $[Ag^{I}(TTM)_2]^{3-}$ORP* (Figure S1), ^{1}H NMR spectra of apo-ORP* with H_2O_2 (Figure S2), EPR spectra of Cu^{II}-ORP* in Tris-HCl vs phosphate buffer (Figure S3), ^{1}H NMR spectra of Ag^{I} with apo-ORP* (Figure S4), and the gel filtration chromatogram and SDS-PAGE gel (Figure S5) (PDF)

■ AUTHOR INFORMATION

Corresponding Author

*E-mail: jose.moura@fct.unl.pt.

ORCID

Biplab K. Maiti: 0000-0002-0985-0031
Rui M. Almeida: 0000-0003-3517-349X
Luisa B. Maia: 0000-0002-6901-6591
Isabel Moura: 0000-0003-0971-4977
José J. G. Moura: 0000-0002-4726-2388

Notes

The authors declare no competing financial interest.

■ ACKNOWLEDGMENTS

This work was supported by the Unidade de Ciências Biomoleculares Aplicadas-UCIBIO, which is financed by national funds from FCT/MEC (UID/Multi/04378/2013) and co-financed by the ERDF under the PT2020 Partnership Agreement (POCI-01-0145-FEDER-007728). B.K.M., L.B.M., and R.M.A. thank FCT/MEC for the fellowship grants (SFRH/BPD/63066/2009, SFRH/BPD/111404/2015, and SFRH/BPD/80293/2011, respectively), which are financed by national funds and co-financed by FSE. The NMR spectrometers are part of the National NMR Network (RNRMN) and are funded by FCT/MEC (project RECI/BBB-BQB/0230/2012).

■ REFERENCES

(1) George, G. N.; Pickering, I. J.; Yu, E. Y.; Prince, R. C.; Bursakov, S. A.; Gavel, O.; Moura, I.; Moura, J. J. G. A Novel Protein-Bound Copper−Molybdenum Cluster. *J. Am. Chem. Soc.* **2000**, *122*, 8321−8322.

(2) Fiévet, A.; My, L.; Cascales, E.; Ansaldi, M.; Pauleta, S. R.; Moura, I.; Dermoun, Z.; Bernard, C. S.; Dolla, A.; Aubert, C. The Anaerobe-Specific Orange Protein Complex of Desulfovibrio vulgaris Hildenborough Is Encoded by Two Divergent Operons Coregulated by σ54 and a Cognate Transcriptional Regulato. *J. Bacteriol.* **2011**, *193*, 3207−3219.

(3) Maiti, B. K.; Moura, I.; Moura, J. J. G.; Pauleta, S. R. The small iron-sulfur protein from the ORP operon binds a [2Fe-2S] cluster. *Biochim. Biophys. Acta, Bioenerg.* **2016**, *1857*, 1422−1429.

(4) Carepo, M. S.; Carreira, C.; Grazina, R.; Zakrzewska, M. E.; Dolla, A.; Aubert, C.; Pauleta, S. R.; Moura, J. J. G.; Moura, I. Orange protein from Desulfovibrio alaskensis G20: insights into the Mo-Cu cluster protein-assisted synthesis. *JBIC, J. Biol. Inorg. Chem.* **2016**, *21*, 53−62.

(5) Carepo, M. S.; Pauleta, S. R.; Wedd, A. G.; Moura, J. J.; Moura, I. Mo-Cu metal cluster formation and binding in an orange protein isolated from Desulfovibrio gigas. *JBIC, J. Biol. Inorg. Chem.* **2014**, *19*, 605−614.

(6) Maiti, B. K.; Maia, L. B.; Pauleta, S. R.; Moura, I.; Moura, J. J. G. Protein-Assisted Formation of Molybdenum Heterometallic Clusters: Evidence for the Formation of S2MoS2-M-S2MoS2 Clusters with M = Fe, Co, Ni, Cu, or Cd within the Orange Protein. *Inorg. Chem.* **2017**, *56*, 2210−2220.

(7) Arnesano, F.; Banci, L.; Bertini, I.; Cantini, F.; Ciofi-Baffoni, S.; Huffman, D. L.; O'Halloran, T. V. Characterization of the binding interface between the copper chaperone Atx1 and the first cytosolic domain of Ccc2 ATPase. *J. Biol. Chem.* **2001**, *276*, 41365−41376.

(8) Banci, L.; Bertini, I.; Ciofi-Baffoni, S.; Kandias, N. G.; Robinson, N. J.; Spyroulias, G. A.; Su, X.-C.; Tottey, S.; Vanarotti, M. The delivery of copper for thylakoid import observed by NMR. *Proc. Natl. Acad. Sci. U. S. A.* **2006**, *103*, 8320−8325.

(9) Banci, L.; Bertini, I.; Cantini, F.; Felli, I. C.; Gonnelli, L.; Hadjiliadis, N.; Pierattelli, R.; Rosato, A.; Voulgaris, P. The Atx1-Ccc2 complex is a metal-mediated protein-protein interaction. *Nat. Chem. Biol.* **2006**, *2*, 367−368.

(10) Banci, L.; Bertini, I.; Cantini, F.; Ciofi-Baffoni, S. Cellular copper distribution: a mechanistic systems biology approach. *Cell. Mol. Life Sci.* **2010**, *67*, 2563−2589.

(11) Alvarez, H. M.; Xue, Y.; Robinson, C. D.; Canalizo-Hernández, M. A.; Marvin, R. G.; Kelly, R. A.; Mondragón, A.; Penner-Hahn, J. E.; O'Halloran, T. V. Tetrathiomolybdate inhibits copper trafficking proteins through metal cluster formation. *Science* **2010**, *327*, 331−334.

(12) Blackburn, N. J. A Tale of Two Metals. *Chem. Biol.* **2010**, *17*, 8−9.

(13) Chidambaram, M. V.; Barnes, G.; Frieden, E. Inhibition of ceruloplasmin and other copper oxidases by thiomolybdate. *J. Inorg. Biochem.* **1984**, *22*, 231−239.

(14) Bissig, K. D.; Voegelin, T. C.; Solioz, M. Tetrathiomolybdate inhibition of the Enterococcus hirae CopB copper ATPase. *FEBS Lett.* **2001**, *507*, 367−370.

(15) Pufahl, R. A.; Singer, C. P.; Peariso, K. L.; Lin, S. J.; Schmidt, P. J.; Fahrni, C. J.; Culotta, V. C.; Penner-Hahn, J. E.; O'Halloran, T. V. Metal ion chaperone function of the soluble Cu(I) receptor Atx1. *Science* **1997**, *278*, 853−856.

(16) Huffman, D. L.; O'Halloran, T. V. Energetics of Copper Trafficking between the Atx1Metallochaperone and the Intracellular Copper Transporter, Ccc2. *J. Biol. Chem.* **2000**, *275*, 18611−18614.

(17) Brewer, G. J. Raulin award lecture: Wilson's disease therapy with zinc and tetrathiomolybdate. *J. Trace Elem. Exp. Med.* **2000**, *13*, 51−61.

(18) Zhang, L.; Lichtmannegger, J.; Summer, K. H.; Webb, S.; Pickering, I. J.; George, G. N. Tracing Copper−Thiomolybdate Complexes in a Prospective Treatment for Wilson's Disease. *Biochemistry* **2009**, *48*, 891−897.

(19) George, G. N.; Pickering, I. J.; Harris, H. H.; Gailer, J.; Klein, D.; Lichtmannegger, J.; Summer, K.-H. Tetrathiomolybdate causes formation of hepatic copper-molybdenum clusters in an animal model of Wilson's disease. *J. Am. Chem. Soc.* **2003**, *125*, 1704−1705.

(20) Lee, V. E.; Schulman, J. M.; Stiefel, E. I.; Lee, C. C. Reversible precipitation of bovine serum albumin by metal ions and synthesis, structure and reactivity of new tetrathiometallate chelating agents. *J. Inorg. Biochem.* **2007**, *101*, 1707−1718.

(21) Jiang, J.; Nadas, I. A.; Kim, M. A.; Franz, K. J. A Mets Motif Peptide Found in Copper Transport Proteins Selectively Binds Cu(I) with Methionine-Only Coordination. *Inorg. Chem.* **2005**, *44*, 9787−9794.

(22) Haas, K. L.; Putterman, A. B.; White, D. R.; Thiele, D. J.; Franz, K. J. Model peptides provide new insights into the role of histidine

DOI: 10.1021/acs.inorgchem.7b00840
Inorg. Chem. 2017, 56, 8900−8911

residues as potential ligands in human cellular copper acquisition via Ctr1. *J. Am. Chem. Soc.* **2011**, *133*, 4427−4437.
(23) Rubino, J. T.; Chenkin, M. P.; Keller, M.; Riggs-Gelasco, P.; Franz, K. J. A comparison of methionine, histidine and cysteine in copper(I)-binding peptides reveals differences relevant to copper uptake by organisms in diverse environments. *Metallomics* **2011**, *3*, 61−73.
(24) Cabras, T.; Patamia, M.; Melino, S.; Inzitari, R.; Messana, I.; Castagnola, M.; Petruzzelli, R. Pro-oxidant activity of histatin 5 related Cu(II)-model peptide probed by mass spectrometry. *Biochem. Biophys. Res. Commun.* **2007**, *358*, 277−284.
(25) Kolozsi, A.; Jancsó, A.; Nagy, N. V.; Gajda, T. *J. Inorg. Biochem.* **2009**, *103*, 940−947.
(26) Harford, C.; Sarkar, B. Amino Terminal Cu(II)- and Ni(II)-Binding (ATCUN) Motif of Proteins and Peptides: Metal Binding, DNA Cleavage, and Other Properties. *Acc. Chem. Res.* **1997**, *30*, 123−130.
(27) Melino, S.; Gallo, M.; Trotta, E.; Mondello, F.; Paci, M.; Petruzzelli, R. Metal-Binding and Nuclease Activity of an Antimicrobial Peptide Analogue of the Salivary Histatin 5. *Biochemistry* **2006**, *45*, 15373−15383.
(28) Bal, W.; Wójcik, J.; Maciejczyk, M.; Grochowski, P.; Kasprzak, K. S. Induction of a Secondary Structure in the N-Terminal Pentadecapeptide of Human Protamine HP2 through Ni(II) Coordination. An NMR Study. *Chem. Res. Toxicol.* **2000**, *13*, 823−830.
(29) Mal, T. K.; Ikura, M.; Kay, L. E. The ATCUN Domain as a Probe of Intermolecular Interactions: Application to Calmodulin−Peptide Complexes. *J. Am. Chem. Soc.* **2002**, *124*, 14002−14003.
(30) Donaldson, L. W.; Skrynnikov, N. R.; Choy, W.-Y.; Muhandiram, D. R.; Sarkar, B.; Forman-Kay, J. D.; Kay, L. E. Structural Characterization of Proteins with an Attached ATCUN Motif by Paramagnetic Relaxation Enhancement NMR Spectroscopy. *J. Am. Chem. Soc.* **2001**, *123*, 9843−9847.
(31) Gaponenko, V.; Dvoretsky, A.; Walsby, C.; Hoffman, B. M.; Rosevear, P. R. Calculation of z-Coordinates and Orientational Restraints Using a Metal Binding Tag. *Biochemistry* **2000**, *39*, 15217−15224.
(32) Brath, U.; Swamy, S. I.; Veiga, A. X.; Tung, C.-C.; Ven Petegem, F.; Erdélyi, M. Paramagnetic Ligand Tagging To Identify Protein Binding Sites. *J. Am. Chem. Soc.* **2015**, *137*, 11391−11398.
(33) Otting, G. Protein NMR using paramagnetic ions. *Annu. Rev. Biophys.* **2010**, *39*, 387−405.
(34) Pauleta, S. R.; Duarte, A. G.; Carepo, M. S.; Pereira, A. S.; Tavares, P.; Moura, I.; Moura, J. J. NMR assignment of the apo-form of a Desulfovibrio gigas protein containing a novel Mo-Cu cluster. *Biomol. NMR Assignments* **2007**, *1*, 81−83.
(35) Najmudin, S.; Bonifácio, C.; Duarte, A. G.; Pauleta, S. R.; Moura, I.; Moura, J. J. G.; Romão, M. J. Crystallization and crystallographic analysis of the apo form of the orange protein (ORP) from Desulfovibrio gigas. *Acta Crystallogr., Sect. F: Struct. Biol. Cryst. Commun.* **2009**, *65*, 730−732.
(36) Lowry, O. H.; Rosebrough, N. J.; Farr, A. L.; Randall, R. J. Protein Measurement With the Folin Phenol Reagent. *J. Biol. Chem.* **1951**, *193*, 265−275.
(37) Keller, R. *The Computer Aided Resonance Assignment Tutorial*; Cantina Verlag: Goldau, Switzerland, 2004.
(38) Garrett, D. S.; Seok, Y. J.; Peterkofsky, A.; Clore, G. M.; Gronenborn, A. M. Identification by NMR of the Binding Surface for the Histidine-Containing Phosphocarrier Protein HPr on the N-Terminal Domain of Enzyme I of the Escherichia coli Phosphotransferase System. *Biochemistry* **1997**, *36*, 4393−4398.
(39) Dominguez, C.; Boelens, R.; Bonvin, A. M. J. J. HADDOCK: A Protein−Protein Docking Approach Based on Biochemical or Biophysical Information. *J. Am. Chem. Soc.* **2003**, *125*, 1731−1737.
(40) Wassenaar, T. A.; et al. WeNMR: Structural Biology on the Grid. *J. Grid. Comp.* **2012**, *10*, 743−767.
(41) Pettersen, E. F.; Goddard, T. D.; Huang, C. C.; Couch, G. S.; Greenblatt, D. H.; Meng, E. C.; Ferrin, T. E. UCSF Chimera—A visualization system for exploratory research and analysis. *J. Comput. Chem.* **2004**, *25*, 1605−1612.
(42) (a) Vangone, A.; Bonvin, A. M. J. J. Contacts-based prediction of binding affinity in protein−protein complexes. *eLife* **2015**, *4*, e07454. (b) Xue, L.; Rodrigues, J.; Kastritis, P.; Bonvin, A. M. J. J.; Vangone, A. PRODIGY: a web server for predicting the binding affinity of protein-protein complexes. *Bioinformatics* **2016**, *32*, 3676−3678.
(43) Bortolus, M.; Bisaglia, M.; Zoleo, A.; Fittipaldi, M.; Benfatto, M.; Bubacco, L.; Maniero, A. L. Structural Characterization of a High Affinity Mononuclear Site in the Copper(II)-α-Synuclein Complex. *J. Am. Chem. Soc.* **2010**, *132*, 18057−18066.
(44) Sundberg, R. J.; Martin, R. B. Interactions of histidine and other imidazole derivatives with transition metal ions in chemical and biological systems. *Chem. Rev.* **1974**, *74*, 471−517.
(45) Kim, M. K.; Martell, A. E. Copper(II) Complexes of Triglycine and Tetraglycine. *J. Am. Chem. Soc.* **1966**, *88*, 914−918.
(46) Sigel, H.; Martin, R. B. Coordinating properties of the amide bond. Stability and structure of metal ion complexes of peptides and related ligands. *Chem. Rev.* **1982**, *82*, 385−426.
(47) Shenberger, Y.; Gottlieb, H. E.; Ruthstein, S. EPR NMR spectroscopies provide input on the coordination of Cu(I) and Ag(I) to a disordered methionine segment. *JBIC, J. Biol. Inorg. Chem.* **2015**, *20*, 719−727.
(48) Rubino, J. T.; Riggs-Gelasco, P.; Franz, K. J. Methionine motifs of copper transport proteins provide general and flexible thioether-only binding sites for Cu(I) and Ag(I). *JBIC, J. Biol. Inorg. Chem.* **2010**, *15*, 1033−1049.
(49) Müller, A.; et al. Darstellung und Röntgenstrukturanalyse von 26 Thiomolybdato- bzw. Thiowolframato-und eines Selenowolframato-Komplexes. *Monatsh. Chem.* **1989**, *120*, 367−391.
(50) Müller, A.; Diemann, E.; Jostes, D.-C. R.; Bögge, H. Transition Metal Thiometalates: Properties and Significance in Complex and Bioinorganic Chemistry. *Angew. Chem., Int. Ed. Engl.* **1981**, *20*, 934−955.
(51) Ciriolo, M. R.; Civitareale, P.; Carrì, M. T.; Martino, A.; Galiazzo, F.; Rotilio, G. Purification and characterization of Ag,Zn-superoxide dismutase from Saccharomyces cerevisiae exposed to silver. *J. Biol. Chem.* **1994**, *269*, 25783−25787.
(52) Singh, S. K.; Roberts, S. A.; McDevitt, S. F.; Weichsel, A.; Wildner, G. F.; Grass, G. B.; Rensing, C.; Montfort, W. R. Crystal structures of multicopper oxidase CueO bound to copper(I) and silver(I): functional role of a methionine-rich sequence. *J. Biol. Chem.* **2011**, *286*, 37849−37857.
(53) Viles, J. H.; Cohen, F. E.; Prusiner, S. B.; Goodin, D. B.; Wright, P. E.; Dyson, H. J. Copper binding to the prion protein: Structural implications of four identical cooperative binding sites. *Proc. Natl. Acad. Sci. U. S. A.* **1999**, *96*, 2042−2047.
(54) Kalverda, A. P.; Salgado, J.; Dennison, C.; Canters, G. W. Analysis of the Paramagnetic Copper(II) Site of Amicyanin by 1H NMR Spectroscopy. *Biochemistry* **1996**, *35*, 3085−3092.
(55) Laussac, J. P.; Sarker, B. Characterization of the copper(II) and nickel(II) transport site of human serum albumin. Studies of copper(II) and nickel(II) binding to peptide 1−24 of human serum albumin by carbon-13 and proton NMR spectroscopy. *Biochemistry* **1984**, *23*, 2832−2838.
(56) Pushie, M. J.; Shaw, K.; Franz, K. J.; Shearer, J.; Haas, K. L. Model Peptide Studies Reveal a Mixed Histidine-Methionine Cu(I) Binding Site at the N-Terminus of Human Copper Transporter 1. *Inorg. Chem.* **2015**, *54*, 8544−8551.
(57) NMR assignment of the apo-form of a Desulfovibrio gigas ORP, rest.bmrb.wisc.edu/bmrb/NMR-STAR3/15200.
(58) Nadal, R. C.; Abdelraheim, S. R.; Brazier, M. W.; Rigby, S. E. J.; Brown, D. R.; Viles, J. H. Prion protein does not redox-silence Cu2+, but is a sacrificial quencher of hydroxyl radicals. *Free Radical Biol. Med.* **2007**, *42*, 79−89.
(59) Jacob, C.; Giles, G. I.; Giles, N. M.; Sies, H. Sulfur and selenium: the role of oxidation state in protein structure and function. *Angew. Chem., Int. Ed.* **2003**, *42*, 4742−4758.

DOI: 10.1021/acs.inorgchem.7b00840
Inorg. Chem. 2017, 56, 8900−8911

(60) Kirn, J.; Rees, D. C. Crystallographic structure and functional implications of the nitrogenase molybdenum−iron protein from Azotobacter vinelandii. *Nature* **1992**, *360*, 553−560.
(61) Neca, A. J.; Soares, R.; Carepo, M. S. P.; Pauleta, S. R. Resonance assignment of DVU2108 that is part of the Orange Protein complex in Desulfovibrio vulgaris Hildenborough. *Biomol. NMR Assignments* **2016**, *10*, 117−120.
(62) Cort, J. R.; Yee, A.; Edwards, A. M.; Arrowsmith, C. H.; Kennedy, M. A. NMR structure determination and structure-based functional characterization of conserved hypothetical protein MTH1175 from Methanobacterium thermoautotrophicum. *J. Struct. Funct. Genomics* **2000**, *1*, 15−25.
(63) Peisach, J.; Blumberg, W. E. Structural implications derived from the analysis of electron paramagnetic resonance spectra of natural and artificial copper proteins. *Arch. Biochem. Biophys.* **1974**, *165*, 691−708.
(64) Solomon, E. I.; Lowery, M. D.; LaCroix, L. B.; Root, D. E. [1] Electronic absorption spectroscopy of copper proteins. *Methods Enzymol.* **1993**, *226*, 1−33.
(65) Bryce, G. F.; Gurd, F. R. N. Visible Spectra and Optical Rotatory Properties of Cupric Ion Complexes of L-Histidine-containing Peptides. *J. Biol. Chem.* **1966**, *241*, 122−129.
(66) Zoroddu, M. A.; Medici, S.; Peana, M. Copper and nickel binding in multi-histidinic peptide fragments. *J. Inorg. Biochem.* **2009**, *103*, 1214−1220.
(67) Hureau, C.; Eury, H.; Guillot, R.; Bijani, C.; Sayen, S.; Solari, P.-L.; Guillon, E.; Faller, P.; Dorlet, P. X-ray and Solution Structures of CuIIGHK and CuIIDAHK Complexes: Influence on Their Redox Properties. *Chem. - Eur. J.* **2011**, *17*, 10151−10160.
(68) Neupane, K. P.; Aldous, A. R.; Kritzer, J. A. Macrocyclization of the ATCUN Motif Controls Metal Binding and Catalysis. *Inorg. Chem.* **2013**, *52*, 2729−2735.
(69) Bai, Y.; Luo, Q.; Liu, J. Protein self-assembly via supramolecular strategies. *Chem. Soc. Rev.* **2016**, *45*, 2756−2767.
(70) Hoskins, J.; Lovell, S.; Blundell, T. L. An algorithm for predicting protein−protein interaction sites: Abnormally exposed amino acid residues and secondary structure elements. *Protein Sci.* **2006**, *15*, 1017−1029.
(71) Abriata, L. A.; Banci, L.; Bertini, I.; Ciofi-Baffoni, S.; Gkazonis, P.; Spyroulias, G. A.; Vila, A. J.; Wang, S. Mechanism of CuA assembly. *Nat. Chem. Biol.* **2008**, *4*, 599−601.
(72) Pelzmann, A. M.; Mickoleit, F.; Meyer, O. Insights into the posttranslational assembly of the Mo-, S- and Cu-containing cluster in the active site of CO dehydrogenase of Oligotropha carboxidovorans. *JBIC, J. Biol. Inorg. Chem.* **2014**, *19*, 1399−1414.
(73) Dos Santos, P. C.; Dean, D. R.; Hu, Y.; Ribbe, M. W. Formation and Insertion of the Nitrogenase Iron−Molybdenum Cofactor. *Chem. Rev.* **2004**, *104*, 1159−1174.
(74) Reedijk, J. Plasticity in the copper−thioether bond: Manifestation in blue Cu proteins and in synthetic analogs. *J. Inorg. Biochem.* **2012**, *115*, 182−185.
(75) Pushie, M. J.; Shaw, K.; Franz, K. J.; Shearer, J.; Haas, K. L. Model Peptide Studies Reveal a Mixed Histidine-Methionine Cu(I) Binding Site at the N-Terminus of Human Copper Transporter 1. *Inorg. Chem.* **2015**, *54*, 8544−8551.
(76) Solomon, E. I.; Baldwin, M. J.; Lowery, M. D. Electronic structures of active sites in copper proteins: contributions to reactivity. *Chem. Rev.* **1992**, *92*, 521−542.
(77) Pearson, R. G. Hard and Soft Acids and Bases. *J. Am. Chem. Soc.* **1963**, *85*, 3533−3539.

DOI: 10.1021/acs.inorgchem.7b00840
Inorg. Chem. 2017, 56, 8900−8911